Errata

EDITOR'S NOTE: The following article originally was published in the July 1976 issue of the *Journal of Spacecraft and Rockets*. Unfortunately in paging this article, sections of text were misplaced. Therefore so that our readers and the authors may have a complete, comprehensible article, we are publishing this article in its entirety.

Experimental Dynamic Stability Characteristics of a Shuttle Orbiter at $M_\infty = 8$

Bob L. Uselton*
ARO, Inc., Arnold Engineering Development Center, Arnold Air Force Station, Tenn.
and
Delma C. Freeman Jr.† and Richmond P. Boyden‡
NASA Langley Research Center, Hampton, Va.

Wind tunnel tests were conducted to measure the pitch, yaw, and roll-damping characteristics of an early shuttle orbiter configuration. Data were obtained utilizing the small amplitude forced-oscillation technique at angles of attack of −4.9 to 26.5 deg at Reynolds numbers, based on model length, of 1.18×10^6 to 4.82×10^6. The orbiter was dynamically stable in pitch, yaw, and roll, and the pitch derivatives were dependent on Reynolds number while the roll derivatives were independent of Reynolds number.

Nomenclature

A = reference area, model wing area, 0.387 ft^2
b = reference length for lateral coefficients, wing span, 0.937 ft
C_ℓ = rolling-moment coefficient, rolling moment/$q_\infty Ab$
C_{ℓ_p} = rolling-moment coefficient due to roll velocity $\partial(C\ell)/\partial(pb/2V_\infty)$, radian^{-1}
$C_{\ell_{\dot\beta}}$ = rolling-moment coefficient due to rate of change of sideslip angle, $\partial(C_\ell)/\partial(\dot\beta b/2V_\infty)$, radian^{-1}
C_m = pitching-moment coefficient, pitching moment/$q_\infty A\bar c$
C_{m_q} = pitching-moment coefficient due to pitch velocity, $\partial(Cm)/\partial(q\bar c/2V_\infty)$, radian^{-1}
C_{m_α} = pitching-moment coefficient due to angle of attack, $\partial(C_m)/\partial\alpha$, radian^{-1}
$C_{m_{\dot\alpha}}$ = pitching-moment coefficient due to rate of change of angle of attack, $\partial(C_m)/\partial(\dot\alpha\bar c/2V_\infty)$, radian^{-1}
C_N = normal-force coefficient, normal force/$q_\infty A$
C_n = yawing-moment coefficient, yawing moment/$q_\infty Ab$
C_{n_p} = yawing-moment coefficient due to roll rate $\partial(C_n)/\partial(pb/2V_\infty)$, radian^{-1}
C_{n_r} = yawing-moment coefficient due to yaw velocity, $\partial(C_n)/\partial(rb/2V_\infty)$, radian^{-1}
C_{n_β} = yawing-moment coefficient due to sideslip angle, $\partial(C_n)/\partial\beta$, radian^{-1}
$C_{n_{\dot\beta}}$ = yawing-moment coefficient due to rate of change of sideslip angle, $\partial(C_n)/\partial(\dot\beta b/2V_\infty)$, radian^{-1}
C_Y = side-force coefficient, side force/$q_\infty A$
C_{Y_p} = side-force coefficient due to roll velocity, $\partial(C_Y)/\partial(pb/2V_\infty)$, radian^{-1}
$C_{Y_{\dot\beta}}$ = side-force coefficient due to rate of change of sideslip angle, $\partial(C_Y)/\partial(\dot\beta b/2V_\infty)$, radian^{-1}
$\bar c$ = reference length for longitudinal coefficients, wing mean aerodynamic chord, 0.475 ft
ℓ = model length (reference length for Reynolds number), 1.290 ft
M_∞ = freestream Mach number
p = rolling velocity, radians/sec
p_0 = tunnel stilling chamber pressure, psia
q = pitching velocity, radians/sec
q_∞ = tunnel freestream dynamic pressure, psfa or psia
Re_ℓ = tunnel freestream Reynolds number based on model length(ℓ)
r = yawing velocity, radians/sec
T_0 = tunnel stilling chamber temperature, ^0R
V_∞ = tunnel freestream velocity, ft/sec
α = angle of attack, deg or radian
β = sideslip angle, radian
$\Delta(\ )$ = uncertainty band (95% confidence limit)
θ,ϕ,ψ = angular displacement in pitch, roll, and yaw, respectively, deg
ω = model angular oscillation frequency, radians/sec
$\omega b/2V_\infty$ = reduced frequency parameter for the yaw- and roll-damping tests, radian
$\omega\bar c/2V_\infty$ = reduced frequency parameter for the pitch-damping tests, radian
$(\dot{})$ = first derivative with respect to time

Introduction

PREVIOUS test programs have been conducted to measure the dynamic derivatives of the shuttle orbiter. The majority of these programs have been conducted at Mach numbers from 0.3 through 4.6.[1,2] In order to extend the range of measured derivatives into the hypersonic speed regime, a test program[3] was conducted at the von Karman Gas Dynamics Facility (VKF). The damping data measured in the

Presented as Paper 75-1026 at the AIAA 1975 Aircraft Systems and Technology Meeting, Los Angeles, Calif., Aug. 4-7, 1975; submitted Sept. 8, 1975; revision received Jan. 22, 1976. The work reported herein was conducted by the Arnold Engineering Development Center (AEDC), Air Force Systems Command (AFSC), for NASA Langley Research Center. The results presented herein were obtained by personnel of ARO, Inc., contract operator of AEDC.

Index categories: Aircraft Aerodynamics (including Component Aerodynamics); Spacecraft Ground Testing and Simulation; (including Components).

*Project Engineer, Aerodynamics Projects Branch, von Karman Gas Dynamics Facility. Member AIAA.

†Aerospace Engineer, Space Systems Division, NASA Langley. Member AIAA.

‡Aerospace Engineer, Subsonic Transonic Aerodynamics Division, NASA Langley. Member AIAA.

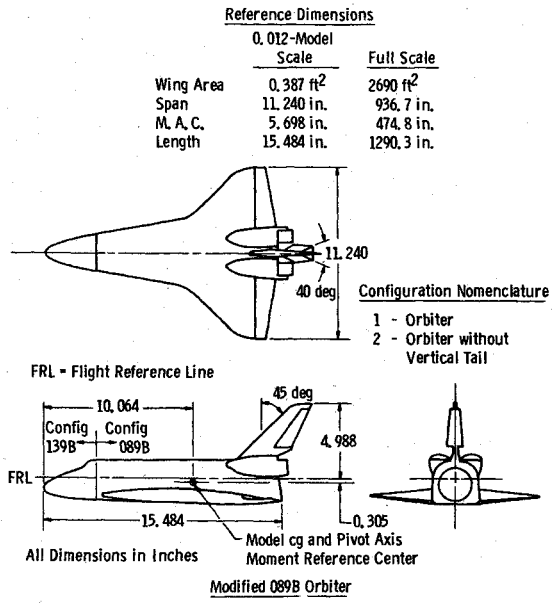

Fig.1 Model details.

previous tests, combined with the present results, have provided the only measured damping data for the shuttle development program. These results have been the basis for the data presented in the shuttle aerodynamic data books, and in turn have been used in the many flight simulations performed to date.

The purpose of the present test program was to measure the pitch, yaw, and roll-damping derivatives of a shuttle orbiter configuration at Mach number 8. The test configuration was a 0.012-scale model of a modified 089B orbiter. Data were obtained at Reynolds number (based on model length) from 1.18×10^6 through 4.82×10^6. The angle of attack was varied from -4.9 to 26.5 deg, and values of the reduced frequency parameter varied from 0.0033 to 0.011. The small-amplitude forced-oscillation technique was utilized.

Apparatus

Model

The modification to the model consisted of using a 139B nose on the 089B body (see Fig. 1). Tests were conducted with body flap off (because of interference with sting), the rudder flare angle = 40 deg, and the elevons set at zero (configuration 1). The orbiter was also tested without the vertical tail(con-

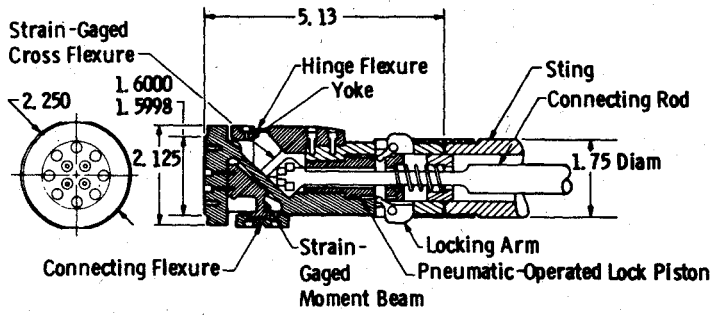

Fig.2 Pitch-yaw-damping test mechanism (VKF 1.B).

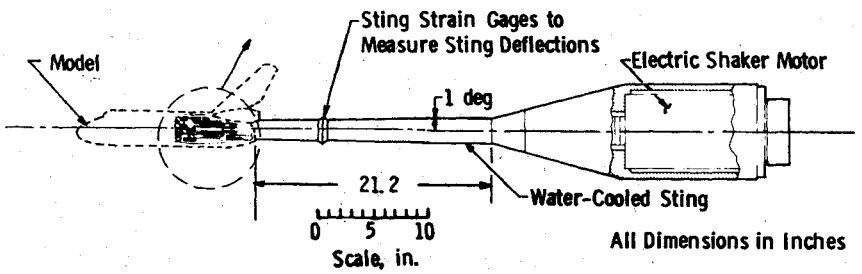

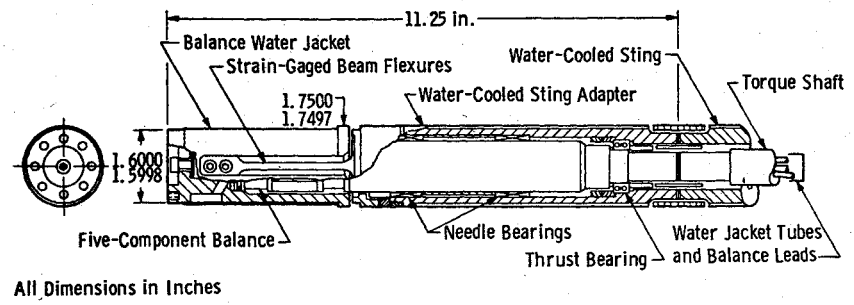

Fig.3 Roll-damping test mechanism (VKF 1.D).

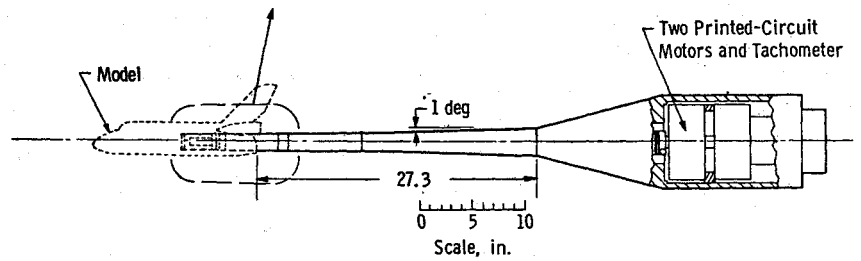

figuration 2). The configurations were balanced about the flexure pivot axis for the pitch tests and about the roll axis for the roll tests. Model details are shown in Fig. 1.

Test Mechanism

Pitch-/ Yaw-Damping Mechanism

The VKF 1. B pitch-yaw-damping test mechanism (Fig.2) utilizes a crossflexure pivot, an electric shaker motor, and a one-component moment beam which is instrumented with strain gages to measure the forcing moment of the shaker motor. The motor is coupled to the moment beam by means of a connecting rod and flexural linkage. The cross flexures, which are instrumented to measure the pitch/yaw displacement, support the model loads and provide the restoring moment to cancel the inertia moment when the system is operating at its natural frequency. A pneumatic and spring-operated locking device is provided to hold the model during injection into, or retraction from the tunnel, or during tunnel starts. A water-cooled sting was used in conjunction with a 132 ft-lb/radian cross-flexure balance and a ±3 in.-lb moment beam. Further details of the test mechanism may be found in Ref. 4.

Roll-Damping Mechanism

The VKF 1.D roll-damping test mechanism (Fig. 3) utilizes a water-jacketed, five-component balance, twin beam flexures, roller bearings to support the loads, and two electric printed-circuit drive motors. The motors are directly coupled to the balance, and the twin beam flexures provide a restoring moment which cancels the inertia moment when the system is operating at the natural frequency of the model-flexure system. The flexures are instrumented to measure the roll displacement.

The balance utilized outrigger beams in the yaw sections and thin-ribbed flexures in the roll section to provide sensitive yaw and roll outputs while maintaining large normal-force capacity and rigidity in yaw. Semi-conductor gages are also utilized for the yaw and roll sections for additional sensitivity. A detailed description of the mechanism can be found in Ref.5. The −59 balance used has the load capacity listed as follows: normal force, 500 lb; pitching-moment, 1125 in.-lb; side force, 40 lb; yawing moment, 84 in.-lb; rolling moment, 10 in.-lb.

Instrumentation

The forced-oscillation instrumentation utilizes an electronic analog system with precision electronics. The control, monitor, and data acquisition instrumentation is contained in a portable console that can be easily interfaced with the instrumentation of the various tunnels.

The control instrumentation provides a system which can vary the oscillation frequency, oscillation amplitude, and angular position (θ,ψ, or Φ) of the model within the flexure limits. The oscillation amplitude is controlled by an electronic feedback loop which permits testing of both dynamically stable and unstable configurations. Additional information regarding instrumentation and data reduction for both balances may be found in Refs. 4, 5, and 6.

Wind Tunnel

Hypersonic Wind Tunnel (B) is a continuous, closed-circuit, variable density wind tunnel with two axisymmetric contoured nozzles and a 50 in.-diam test section. The tunnel can be operated at a nominal Mach number of 6 or 8 at stagnation pressures from 20 to 300 and 50 to 900 psia, respectively, at stagnation temperatures up to 1350°R.

Procedure and Precision of Data

Test Conditions

The nominal wind tunnel test parameters at which the data were obtained are presented in Table 1, and summaries of test configurations for the pitch, yaw, and roll tests are presented in Table 2.

Table 1 Tunnel conditions for pitch-, yaw-, and roll-damping tests

Test Condition	M_∞	$Re_\ell \times 10^{-6}$	p_0, psia	T_0, °R	q_∞, psia	V_∞, ft/sec
A	7.95	1.18	200	1310	0.945	3819
B	7.98	2.35	401	1314	1.862	3826
C	7.99	3.52	600	1308	2.767	3818
D	8.00	4.73	851	1358	3.906	3890
E	8.00	4.82	849	1335	3.894	3857

Table 2 Test summaries

Pitch-Damping Tests

Configuration	Test Condition[a]	$\omega\bar{c}/2V_\infty \times 10^3$	α range, deg
1	D	3.40	24
1	A	3.34	-3.7 to 7.4
1	B	3.34	-4.1 to 25.9
1	E	3.32	-4.9 to 23.9

Yaw-Damping Tests

Configuration	Test Condition[a]	$\omega b/2V_\infty \times 10^3$	α range, deg
1	B	6.27	-3.3 to 25.3
2	B	6.60	-3.4 to 25.3

Roll-Damping Tests

Configuration	Test Condition[a]	$\omega b/2V_\infty \times 10^3$	α range, deg
1	D	10.2	-3.1 to 26.5
1	C	10.4	-2.9 to 26.1
1	B	10.4	-2.5 to 26.0
1	A	10.4	-2.5 to 25.8
2	B	11.0	-2.6 to 26.0
2	D	10.8	-2.6 to 26.2

[a] As defined in Table 1.

Table 3 Tunnel parameters uncertainty

$Re_\ell \times 10^{-6}$	$\Delta(M_\infty)$	$\Delta(Re_\ell \times 10^{-6})$	$\Delta(q_\infty)$ psi	$\Delta(V_\infty)$ fps
1.18	±0.024	±0.011	±0.013	±9.5
2.35	±0.024	±0.022	±0.026	±9.5
3.52	±0.024	±0.033	±0.040	±9.5
4.82	±0.024	±0.045	±0.056	±9.5

Test Procedure

The model was oscillated at a constant oscillation amplitude of ±1 deg for the pitch- and yaw-damping tests, and ±2 deg during the roll-damping tests.

Precision of Data

Uncertainties (bands which include 95% of the calibration data) in the basic tunnel parameters (p_0, T_0, and M_∞) were estimated from repeat calibrations of the instrumentation and from repeatability and uniformity of the test section flow during tunnel calibrations. These uncertainties were used to estimate uncertainties in other freestream properties using a Taylor series method of error propagation.[7]. The estimated uncertainties are shown in Table 3.

Sting bending effects utilizing the technique illustrated in Ref. 8 were used in the data reduction of the pitch- and yaw-damping derivatives. Uncertainties in the measurements of

Table 4 Pitch-damping uncertainty

$Re_\ell \times 10^{-6}$	α,deg	$C_{mq}+C_{m_{\dot\alpha}}$	$\Delta(C_{mq}+C_{m_{\dot\alpha}})$	C_{m_α}	$\Delta(C_{m_\alpha})$
1.18	−0.4	−1.0	±0.13	0.05	±0.026
1.18	7.4	−1.3	±0.13	0.13	±0.026
4.82	2.3	−0.8	±0.04	0.05	±0.006
4.82	23.9	−2.4	±0.06	−0.10	±0.008

Table 5 Yaw-damping uncertainty

$Re_\ell \times 10^{-6}$	α,deg	$C_{n_r}-C_{n_{\dot\beta}}\cos\alpha$	$\Delta(C_{n_r}-C_{n_{\dot\beta}}\cos\alpha)$	$C_{n_\beta}\cos\alpha$	$\Delta(C_{n_\beta}\cos\alpha)$
2.35	0	−0.78	±0.026	−0.04	±0.007
2.35	25.3	−0.23	±0.019	−0.10	±0.007

Table 6 Roll-damping uncertainty

$Re_\ell \times 10^{-6}$	α,deg	$C_{\ell_p}+C_{\ell_{\dot\beta}}\sin\alpha$	$\Delta(C_{\ell_p}+C_{\ell_{\dot\beta}}\sin\alpha)$
1.18	0	−0.11	±0.027
1.18	24	−0.21	±0.028
4.82	0	−0.12	±0.008
4.82	26	−0.24	±0.009

Table 7 Static data uncertainty

$Re_\ell \times 10^{-6}$	$\Delta(C_N)$ [a]	$\Delta(C_N)$ [b]	$\Delta(C_m)$ [a]	$\Delta(C_m)$ [b]
1.18	±0.019	±0.22	±0.010	±0.010
4.82	±0.005	±0.011	±0.002	±0.003

[a] Near minimum values. [b] Near maximum values.

sting effects were included in the error analysis. The uncertainties in the balance and data system were combined with uncertainties in the tunnel parameters assuming a Taylor series method of error propagation[7] to estimate the precision of the aerodynamic damping coefficients. The estimated uncertainties are shown in Tables 4, 5, 6, and 7.

Measurements of the model pitch are precise within ±0.05 deg, based on repeat calibrations. Model attitude corrections were made for model-balance deflections under air load, and the precision of the calculated model angle is estimated to be ±0.1 deg.

Results and Discussion

Figure 4 shows the normal-force and pitching-moment coefficients as a function of angle of attack for configuration 1 (orbiter) and configuration 2 (without vertical tail) at several Reynolds numbers. The normal-force coefficient showed no measurable effect of Reynolds number. The pitching-moment coefficients did show some measurable effect of Reynolds number at $\alpha > 8$ deg. The static data also showed that neither configuration trimmed at the angles of attack tested for the reference center of gravity of this particular configuration.

The pitch-stability derivatives as a function of angle of attack for configuration 1 are shown in Fig. 5 at Reynolds numbers, based on model length of 1.18×10^6, 2.35×10^6, and 4.81×10^6. The orbiter was dynamically stable in pitch, and the damping derivatives generally increased with angle of attack. For $Re_\ell = 2.35\times10^6$ and 4.81×10^6, the slope of the pitching-moment curve showed variation with angle of attack and changed from a positive to negative slope in the 12 to 18 deg angle-of-attack range. The significant Reynolds number effect occurred in the −2 to 2 deg angle-of-attack range where the pitch damping decreased with increasing Reynolds number. The slope of the pitching-moment curve generally became more stabilizing with increasing Reynolds number.

Figure 6 shows the yaw-stability derivatives as a function of angle of attack for configurations 1 and 2 at $Re_\ell = 2.34\times10^6$.

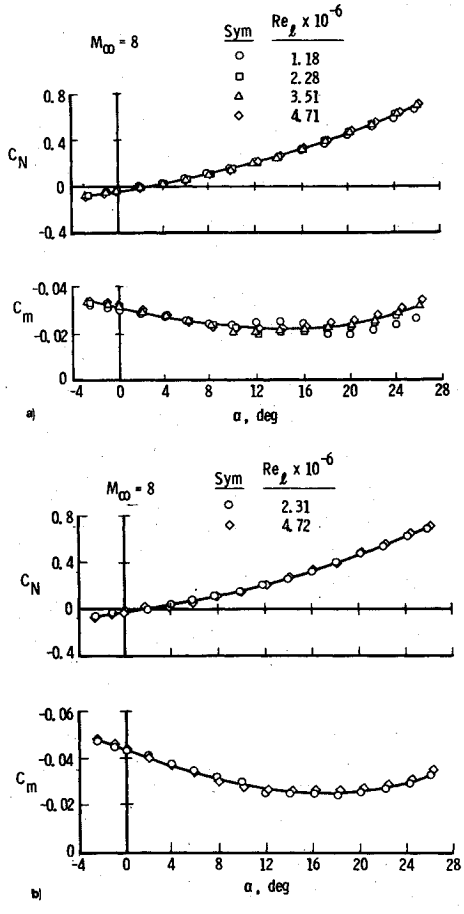

Fig.4 Effect of Reynolds number on the static coefficients. a) Configuration 1. b) Configuration 2 (without vertical tail).

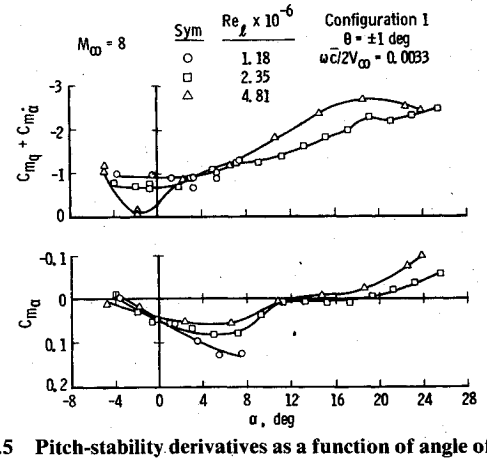

Fig.5 Pitch-stability derivatives as a function of angle of attack.

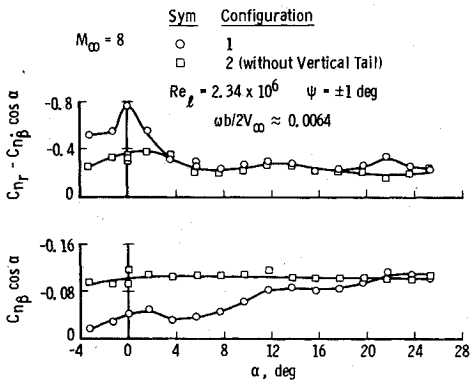

Fig.6 Yaw-stability derivatives as a function of angle of attack.

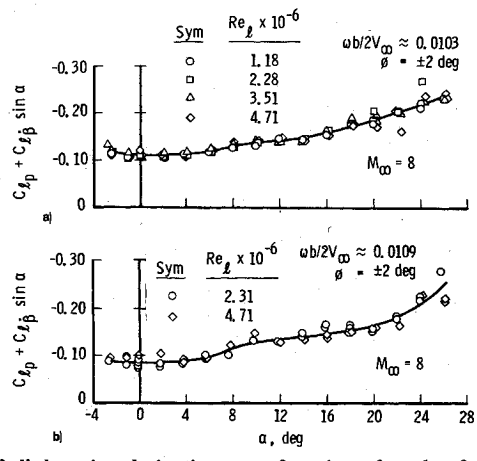

Fig.7 Roll-damping derivatives as a function of angle of attack a) Configuration 1. b) Configuration 2 (without vertical tail).

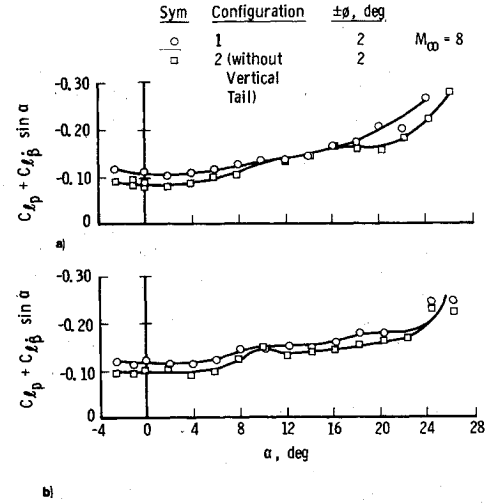

Fig. 8 Effect of vertical tail on the roll-damping derivatives. a) $Re_\ell = 2.3 \times 10^6$. b) $Re_\ell = 4.7 \times 10^6$.

Both configurations were dynamically stable and the damping derivatives were generally invariant for angles of attack above 5 deg. An increase in model damping occurred at the lower angles of attack, particularly for the orbiter configuration. The yawing-moment coefficient due to sideslip angle (C_{n_β} cos α) shows both configurations to be statically unstable in yaw for the moment reference of this particular configuration. Increasing angle of attack increased the static instability of the orbiter and did not affect the instability of the orbiter without the vertical tail (configuration 2). Removal of the vertical tail decreased model damping at the lower angles of attack $-3 \leq \alpha \leq 3$ deg as expected and did not produce any

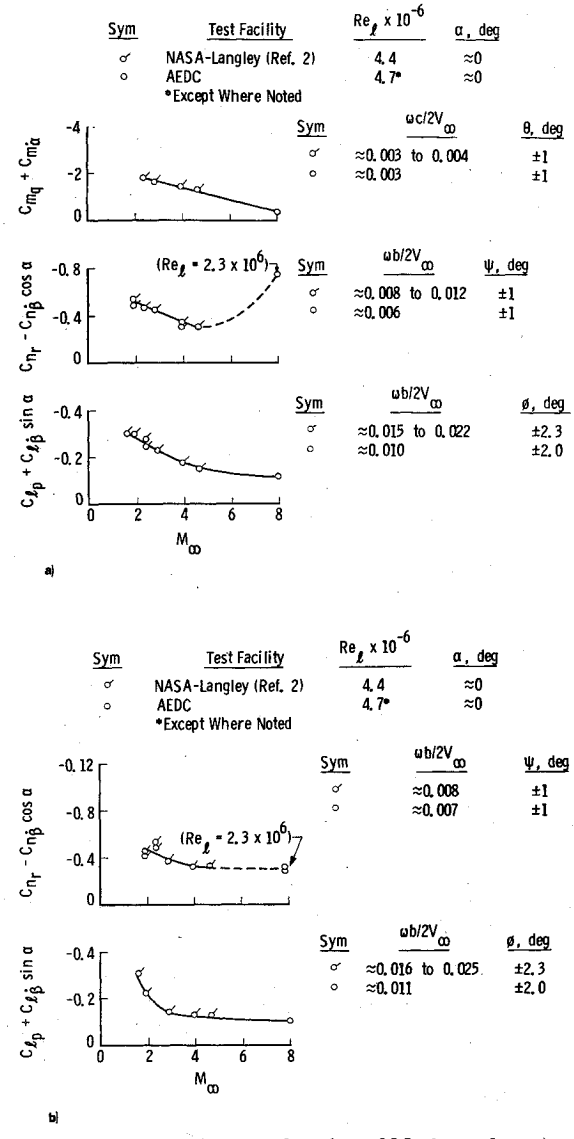

Fig. 9 Damping derivatives as a function of Mach number. a) Configuration 1. b) Configuration 2 (without vertical tail).

large effects for angles of attack greater than 3 deg. For angles of attack up to 20 deg, the static instability increased with the removal of the vertical tail.

The roll-damping derivatives are presented in Fig. 7 for configurations 1 and 2 at several Reynolds numbers. The derivatives generally increased with angle of attack. Varying Reynolds number did not produce any large effects on the roll-damping derivatives. The roll-damping increment due to vertical tail is shown in Fig. 8 for Reynolds numbers 2.3×10^6 and 4.7×10^6. As expected, removing the vertical tail generally decreased model damping slightly.

The pitch-, yaw-, and roll-damping derivatives for configurations 1 and 2 are presented as a function of Mach number for $\alpha = 0$ in Fig. 9. The supersonic data[2] were obtained in the Langley Unitary Plan Wind Tunnel on a 0.0165-scale model. The damping derivatives decreased with increasing Mach number with the exception of the yaw derivatives for configuration 1. The data indicate a significant increase in the yaw damping from the supersonic data at $M_\infty \approx 5$ to the hypersonic data at $M_\infty = 8$ for configuration 1; however, the tail-off data (configuration 2) does not indicate any substantial difference. Thus, the main difference is that the hypersonic data show that the vertical tail adds to the yaw damping at $\alpha = 0$ where the tail is not blocked out by the body wake, while the supersonic data show essentially no effect of

vertical tail on yaw damping. There is a Re_l difference between the two sets of data which may be a contributing factor as was seen in the pitch data (see Fig. 5). Otherwise, no reason for this difference is known.

Conclusions

Wind tunnel tests were conducted to determine the pitch-, yaw-, and roll-damping characteristics of the modified 089B shuttle orbiter configuration. Also, the effect of the vertical tail on the yaw and roll derivatives was investigated. Data were obtained at Mach number 8 at freestream Reynolds numbers, based on model length, of 1.18×10^6 to 4.82×10^6. Conclusions based on the results presented in this report are given below.

1) The orbiter is dynamically stable in pitch, yaw, and roll, and statically unstable in yaw.

2) In general, the pitch- and roll-damping derivatives increase with angle of attack while the yaw-damping derivatives are essentially invariant with angle of attack for $\alpha > 5$ deg.

3) The pitch derivatives of the orbiter are strongly dependent on Reynolds number at the lower angles of attack ($-3 \le \alpha \le 3$ deg) while variation of Reynolds number produces no large effects on the roll-damping derivatives, normal-force coefficients, or pitching-moment coefficients.

4) Removing the vertical tail: (a) decreases the yaw-damping derivatives at the lower angles of attack ($-3 \le \alpha \le 3$ deg); (b) decreases slightly the roll-damping derivatives at the majority of the angles of attack tested; and (c) increases the static instability in yaw.

References

[1] Boyden, R.P. and Freeman, D.C., "Subsonic and Transonic Dynamic Stability of a Modified 089B Shuttle Orbiter," NASA – TMX – 72631, Jan. 1975.

[2] Freeman, D.C., Boyden, R.P., and Davenport, E.E., "Supersonic Dynamic Stability of a Modified 089B Shuttle Orbiter," NASA-TMX-72630, Oct. 1974.

[3] Uselton, B.L. and Jenke, L.M., "Pitch-, Yaw-, and Roll-Damping Characteristics of a Shuttle Orbiter at $M_\infty = 8$," Arnold Engineering Development Center, Arnold AFB, Tenn., AEDC-TR-74-129, May 1975.

[4] Burt, G.E., "A Description of a Pitch/Yaw Dynamic Stability, Forced-Oscillation Test Mechanism for Testing Lifting Configurations," Arnold Engineering Development Center, Arnold AFB, Tenn., AEDC-TR-73-60 (AD762286), June 1973.

[5] Burt, G.E., "A Description of a Forced-Oscillation Test Mechanism for Measuring Dynamic-Stability Derivatives in Roll," Arnold Engineering Development Center, Arnold AFB, Tenn., AEDC-TR-73-49 (AD762258), June 1973.

[6] Schueler, C.J., Ward, L.K., and Hodapp, A.E., Jr., "Techniques for Measurements of Dynamic-Stability Derivatives in Ground Test Facilities," AGARD-ograph 121 (AD669227), Oct. 1967.

[7] Beers, Y., *Introduction to the Theory of Error,* Addison-Wesley, Reading, Mass., 1957, pp. 26-36.

[8] Burt, G.E. and Uselton, J.C., "Effect of Sting Oscillations on the Measurement of Dynamic Stability Derivatives in Pitch and Yaw," *Journal of Aricraft,* Vol. 13, March 1976, pp. 210-216.